Heliyon 5 (2019) e02937

Contents lists available at ScienceDirect

Heliyon

journal homepage: www.cell.com/heliyon

Research article

Isolation and characterization of cellulose and α-cellulose from date palm biomass waste

Emmanuel Galiwango [a], Nour S. Abdel Rahman [a], Ali H. Al-Marzouqi [a,*], Mahdi M. Abu-Omar [b], Abbas A. Khaleel [c]

[a] Department of Chemical and Petroleum Engineering, United Arab Emirates University, P. O. Box 15551, Al Ain, United Arab Emirates
[b] Department of Chemistry and Biochemistry and Biochemistry, UC Santa Barbara, Santa Barbara, CA, 93106-9510, USA
[c] Department of Chemistry, United Arab Emirates University, P. O. Box 15551, Al Ain, United Arab Emirates

ARTICLE INFO

Keywords:
Chemical engineering
Energy
Agriculture
Natural product chemistry
Materials chemistry
Characterization
Isolation
Date palm parts
α-Cellulose
Cellulose

ABSTRACT

Towards the utilization of different parts of date palm biomass waste, low-concentration acid-alkali treatment was used to isolate the contained cellulose and α-cellulose. The cellulose yields achieved from the rachis, leaflet, and fiber parts of the biomass were 74.70%, 71.50%, and 73.82%, respectively, while the corresponding α-cellulose yields were 78.63%, 75.64%, and 70.40%, respectively. The cellulose samples were bleached and characterized by thermogravimetric analysis (TGA), Fourier-transform infrared (FTIR) spectroscopy, scanning electron microscopy (SEM), and X-ray diffraction (XRD). The XRD results revealed high crystallinity of both the cellulose and α-cellulose samples, while the TGA thermograms indicated that the alkali treatment completely removed lignin and hemicelluloses from the rachis. The results of this study demonstrate the promise of using date palm biomass waste as raw material to produce cellulose and α-cellulose.

1. Introduction

Cellulose is the most abundant natural polymer on earth (Zhang and Lynd, 2006; O'Sullivan, 1996) and its proper utilization promises to contribute to sustainable green growth. In the recent past, many researchers have reported the potential use of bio-based renewable natural polymers in biorefineries. An example of such polymers is cellulose, which can be used to produce high-value chemicals, bio-fuel, polymer composites, and many other products like those derived from non-renewable resources such as petroleum (Kumar et al., 2017; Yang et al., 2016; Brinchi et al., 2013; Reyes-Luyanda et al., 2012). Cellulose is present in many plant materials and exists as an insoluble polysaccharide with a polymerization degree of about 10,000. The material consists of linear chains of glucopyranose units linked by β-1,4 glycosidic bonds and has a general formula of $(C_6H_{10}O_5)_n$, where n is the number of repeated monomeric β-d-glucopyranose units and varies with the source of the cellulose (Kumar et al., 2017). Cellulose is the main constituent of a plant cell wall, offering structural support and acting as a reinforcement element together with hemicellulose and lignin. There has been a steady increase in the utilization of cellulose because of its availability in many organisms such as fungi, algae, and bacteria, as well as its low cost, which promises sustainable feed stock supply. Cellulose also has the advantages of being biodegradable, durable, non-toxic, and thermally and mechanically stable. Many studies have been conducted on cellulose derived from different biomass sources as well as commercial source. Prakash et al. (2018) isolated 38% cellulose from a *Mentha arvensis* biomass and used a saccharification process to convert the cellulose into glucose. Szymańska-Chargot et al. (2017) used a fractionation process to characterize cellulose samples derived from apple, tomato, cucumber, and carrot. Through one-pot oxidative-hydrolysis, Chen et al. (2017) achieved a nanostructured cellulose yield of 75.4% from an empty fruit bunch of *Elaeis guineensis*. Other studies have been conducted on the use of different techniques to isolate cellulose from diverse biomass sources such as kenaf fibers and wheat straw (Nuruddin et al., 2016), rice straw (using ionic liquids; Jiang et al., 2011), and wheat straw and soy hull (Alemdar and Sain, 2008).

Date palm biomass waste is rich in cellulose, the exploitation of which promises to contribute to the sustainable development of biorefineries. Palm tree (*Phoenix dactylifera L.*) is considered one of the oldest tree species. Over the last 7,000 years, the plant has been vital to global

* Corresponding author.
E-mail address: hassana@uaeu.ac.ae (A.H. Al-Marzouqi).

https://doi.org/10.1016/j.heliyon.2019.e02937
Received 3 March 2019; Received in revised form 11 July 2019; Accepted 25 November 2019

society, environment, and economy, especially in the Middle East and North Africa in countries like Saudi Arabia, Egypt, UAE, and Algeria (Ahmed et al., 1995). Date palm cultivation is on the increase and its population in the Gulf region has increased over the years. In the UAE, where the present research was conducted, the population of date palm trees stands at about 40 million (Zaid and Helal, 2000). These trees generate tons of waste, much of which is currently converted into compost and used for traditional art and craft or burned, with the accompanying pollution of the environment. Our previous study on the Klason lignin extraction method revealed that the date palm lignocellulosic waste contained in fibers alone consists of cellulose (34%), hemicellulose (17%), and lignin (21%) (Emmanuel et al., 2018). The various parts of date palm waste can thus be used to develop new sustainable bioproducts such as cellulose. This would not only afford great economic and environmental benefits, but also a high-value biomaterial with excellent physical and chemical properties.

However, despite the abundance and rich history of date palm biomass waste in the Middle East, less attention has been given to cellulose and α-cellulose isolation using low concentration acid-alkali treatment method. To the best knowledge of the present authors, there have been few works on the successful isolation and characterization of cellulose and α-cellulose from lignocellulosic sources using dilute acid-alkali treatment process. Acid-alkali treatment is the most effective method for individual cellulose isolation from the complex structure of lignocellulose (Ching and Ng, 2014; Sheltami et al., 2012), and the procedure was thus adopted in the present study. Therefore, the aim of this research is to use low concentration acid-alkaline treatment to isolate cellulose and α-cellulose from date palm waste, characterize it for future applications. Single-component isolation addresses some extrinsic and intrinsic factors that might create problems when the whole complex lignocellulose structure is used in downstream processing (Wu et al., 2016). Wu et al. (2016) investigated the effects of some of these factors in cellulose-lignin interaction during fast pyrolysis.

2. Materials and methods

2.1. Materials

The palm biomass samples were provided by a local farm, having been collected from adult-size (10–15 years old) date palm trees in Al-Ain, UAE (24122 N, 554441 E). The samples were washed with deionized water to remove dust and any other physical impurity, and subsequently dried in a shaded area. All the solvents (ACS grade) and reagents used in the study were purchased from Sigma Aldrich with no further purification applied. The commercial α-cellulose had, molecular weight of (162.1)n (sigma aldrich, 2019). This α-cellulose type was chosen for comparison with isolated α-cellulose sample due to similar applications of aiding extrusion and opacifier, which are important processes considered in our subsequent research for making cutlery from date palm cellulose and biodegradable polymers.

2.2. Preparation of cellulose

Cellulose is physically and chemically surrounded by hemicellulose and lignin, with the links forming a lignocellulose matrix. Pretreatment is thus necessary before an attempt is made to isolate the cellulose. In this study, 10 g of the virgin biomass was sieved through a 250-μm mesh and transferred to a weighing thimble, and then into a Soxhlet flask. The resins, waxes, and other extracts were removed by Soxhlet extraction using benzene/ethanol (2:1) for 5 h. The different parts of the extract-free date palm biomass investigated in this study were similarly treated, unless otherwise stated. The cellulose isolation procedure was as described below.

Five grams of the extract-free biomass sample was weighed into a 250-mL beaker and leached using 200 mL of 0.1 M HCl, with heating at 100 °C and stirring for 2 h. The mixture was then filtered and the insoluble residue rich in cellulose-lignin was washed with 20 mL of deionized water and air dried overnight. The cellulose-lignin-rich residue was then treated with 200 mL of 0.1 M NaOH under constant stirring and heating at 100 °C for 2 h. The mixture was subsequently filtered, and the cellulose-rich residue was washed with 20 mL of a fresh portion of the same 0.1 M NaOH. The cellulose residue was then air-dried overnight prior to bleaching. For the bleaching, the dried isolated cellulose sample was treated using 15, 20, and 10 wt.% acetic acid, hydrogen peroxide, and sulfuric acid, respectively, at 75 °C. The weight of the bleached cellulose expressed as a percentage of the weight of the original biomass sample was considered as the amount of cellulose in the original sample.

The method used to determine the amount of α-cellulose contained in the date palm biomass sample in this study was a modification of that used by John and Royal (1931). Five grams of the extract-free sample was weighed into a 250-mL beaker, which was then placed in a constant-temperature (20 °C) water bath. After the sample attained the temperature of the bath, 17.4% NaOH solution was pipetted into the beaker and the sample was macerated with a stirring glass rod. The NaOH treatment step was repeated and the sample was filtered after 30 min using a Buchner funnel. The residue on the filter paper was oven-dried at 105 °C for 1 h, or until no more change in weight was observed. This was followed by cooling, after which 400 mL of distilled water was added to the sample and the mixture was filtered. The filtration was repeated several times to ensure that all the residues were retained by the filter paper. The residues were then soaked in 100 mL of 20% acetic acid for 10 min, after which the acetic acid was washed off by suction and 1 L of boiling water was added in small portions at a time. The sample was thereafter kept in an oven at 105 °C to remove moisture. The increase in weight of the filter paper expressed as a percentage of the biomass sample was considered as the amount of α-cellulose in the sample.

2.3. Characterization

2.3.1. Chemical composition of date palm waste

In a previous study (Emmanuel et al., 2018), we determined the chemical compositions of different date palm biomass parts using the method prescribed in the American Standard Testing Methods (ASTM) and the Tappi standard method. The weight fractions of the lignocellulose components were determined in triplicates.

2.3.2. Thermogravimetric analysis (TGA)

The thermogravimetric analysis of the palm biomass was conducted using a thermogravimetric analyzer (Q500 series, TA Instrument). A sample of weight 6.0 ± 2.0 mg and heating rates of 10, 15, 20, and 25 °C/min, respectively, were used to analyze the α-cellulose samples, while a ramp rate of 15 °C/min was used to investigate the three date palm parts. All the analysis experiments were performed from 30 to 500 °C, with nitrogen passed at 20 ml/min used as a carrier gas. During the thermodecomposition process, the sample weight was continuously recorded as a function of the temperature and time. A derivative (DTG) curve was used to portray the weight loss of the sample per unit time with respect to the temperature.

2.3.3. Fourier transform infrared (FTIR) spectroscopy

The FTIR analysis was performed using an IRTracer-100 FTIR spectrophotometer (Shimadzu, Kyoto, Japan). The analysis was used to examine the changes in the functional groups induced by the various treatments. The FTIR spectra were recorded on an attenuated total reflection Fourier transform infrared (ATR-FTIR) spectrograph using a range between 400 and 4000 cm^{-1} with an average of 34 scans and a spectral resolution of 4 cm^{-1}.

2.3.4. Scanning electron microscopy (SEM)

A JEOL/EO scanning electron microscope (SEM) operated at 10 kV and a spot size of 40 was used to examine the effect of the acid-alkali cellulose isolation and α-cellulose treatment on the morphology of the

samples. The samples were prepared by placing them on the sample holder and coating them with Au/C using a vacuum sputter coater.

2.3.5. X-ray diffraction (XRD) analysis

The degrees of crystallinity of the isolated cellulose and α-cellulose were determined by the X-ray diffraction method. The samples were scanned using Cu K radiation with the parameters of the working lamp set as follows: $v = 40$ kV, $I = 30$ mA, receiving slit = 0.15 mm. The intensity of the reflections was measured using a scan range of 10–80 and scan speed of 2°/min. The crystallinity index CrI was calculated using the peak intensity method (Segal et al., 1959):

$$CrI = \frac{I_{002} - I_{am}}{I_{002}} \times 100 \quad (1)$$

where I_{002} is the intensity of the peak at $2\theta = 22.5$, and I_{am} is the minimum peak intensity corresponding to the amorphous phase at $2\theta = 18.0°$.

3. Results

3.1. Chemical composition of date palm waste

Effective cellulose isolation requires pretreatment of the biomass to remove the contained resins and waxes and reduce the recalcitrant nature of the lignocellulosic components of the biomass. The pretreatment also solubilizes the lignin and hemicellulose, increasing the cellulose mass fraction in the biomass and its accessibility during the hydrolysis treatment stage.

Figure 1 shows the physical appearance of the isolated cellulose and α-cellulose and a commercial α-cellulose sample. Commercial cellulose was not available in the local market at the time of this study, and the results for the present cellulose samples were therefore compared with those for commercial cellulose available in the literature. As can be observed from Figure 1a, the isolated cellulose was dark brown before bleaching. Not all the parts of the date palm biomass were color-wise affected by the maceration treatment using NaOH. After the two-step bleaching ((b) and (c)) treatment, the color of the sample was changed to off-white. The bleaching process removed the residual lignin in the sample that remained after the acid leaching stage. However, the isolated α-cellulose samples were not bleached, and their color was relatively close to the purchased commercial α-cellulose sample.

The chemical composition of cellulose and isolated cellulose was determined, and the results are summarized in Table 1.

The results in Table 1 indicate that acid-alkaline treatment affords a high cellulose yield. A high α-cellulose yield was also reported by Alemdar and Sain (2008). These high yields of cellulose and α-cellulose reveal the strong potential of date palm biomass as a source of cellulose and a contributor towards green economic growth owing to its cost-effective availability. The results of the material characterization of the obtained celluloses are discussed below.

3.2. Thermogravimetric analysis (TGA)

The thermal characteristics of cellulose can be determined by TGA. Figure 2(A) and (B) shows the thermal degradation thermograms (DTG) and the conversion trends of the celluloses derived from the different date palm parts over a temperature range of 30–500 °C achieved by a heating rate of 15 °C/min.

It can be observed from Figure 2 (A) that the TGA curves of all the celluloses isolated from the different date palm parts reveal similar thermal behaviors. The thermal degradation begins around 200–250 °C, indicating that the isolated cellulose is thermally stable below 200 °C. All the DTG thermograms also have two major peaks; the first peak occurs below 100 °C and represents the evaporation of the moisture adsorbed into the samples, while the second peak occurs between 180 and 350 °C

Table 1. Percentage cellulose contents of the date palm biomass.

Date palm part	Cellulose (lignocellulose)	Isolated cellulose	α-cellulose
Rachis	32.00 ± 1.00	74.70 ± 1.00	78.63 ± 1.00
Leaflet	21.00 ± 2.60	71.50 ± 0.00	75.64 ± 0.00
Fiber	33.00 ± 1.00	73.82 ± 1.00	70.40 ± 1.00

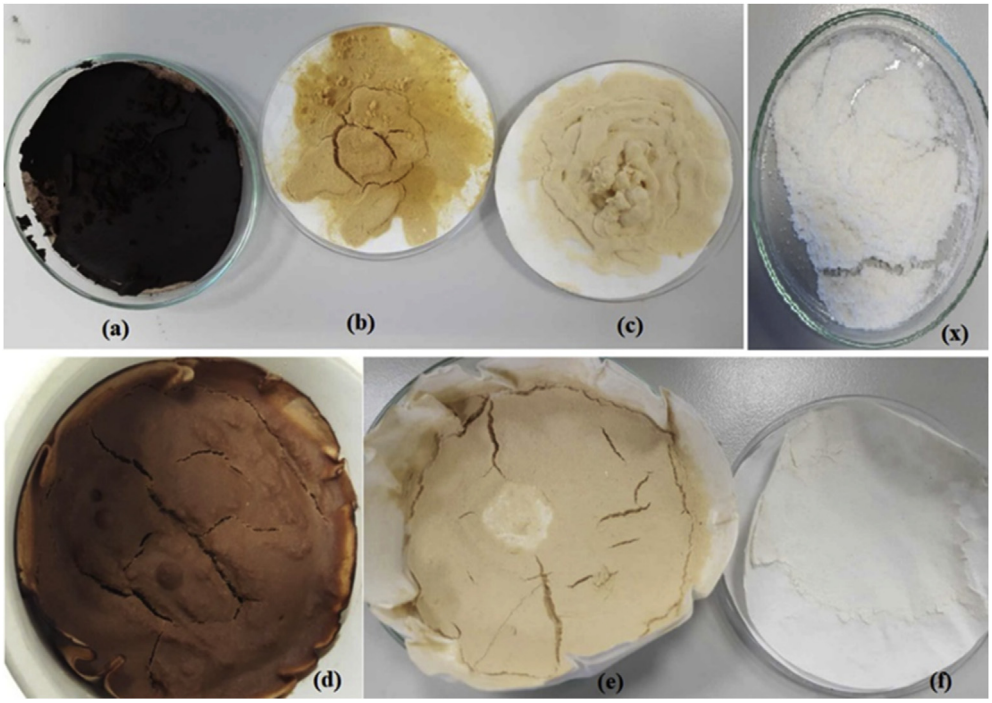

Figure 1. Photographs of (a) the isolated cellulose, (b) the cellulose after the first bleaching (c), the cellulose after the second bleaching; (d)–(f) the unbleached α-cellulose samples; and (X) a commercial α-cellulose sample.

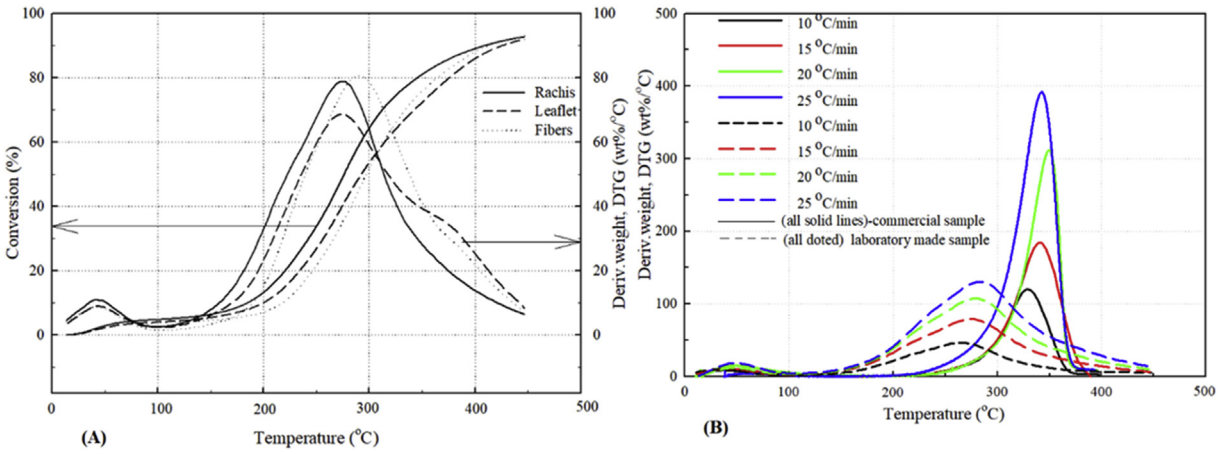

Figure 2. (A) and (B). TGA and DTG curves of celluloses and α-cellulose obtained from different parts of date palm under different heating rates.

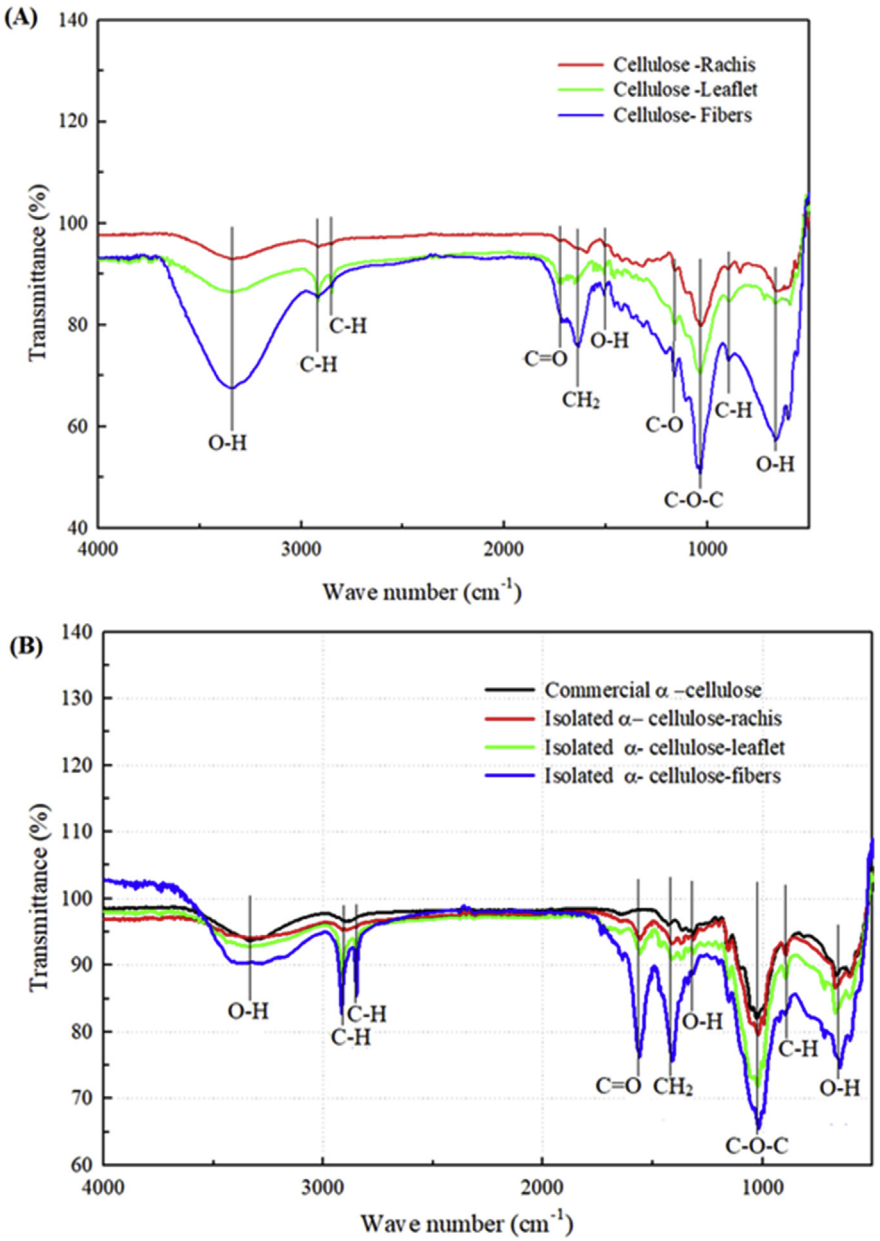

Figure 3. (A) and (B). FTIR spectra of the celluloses α-celluloses isolated from different date palm parts.

and represents the decomposition of the isolated cellulose. Thermal decomposition of cellulose may occur at temperatures within 150–500 °C depending on the biomass source. For example, the cellulose decomposition temperature range is 250–400 °C for *Mentha arvensis* (oil crop) (Prakash et al., 2018), 300–400 °C for commercial microcrystalline cellulose (Loof et al., 2016), 300–360 °C for soybean hull and maize straw (Miranda et al., 2013), and 230–315 °C for cotton, jute, newsprint, and filter paper (Das et al., 2010). Thermal kinetic conversion was also observed to be more favorable for rachis compared with the leaflet and fiber parts; for example, at 300 °C, only 52% conversion was obtained for the leaflet and fiber parts compared with the 62% for rachis. The α-cellulose obtained from rachis was therefore used for the DTG characterization and the results were compared with those for a commercial α-cellulose.

Figure 2 (B) shows the thermal decomposition regimes of the laboratory-made and commercial α-celluloses between temperatures of 30–500 °C as obtained under different heating rates of 10, 15, 20, and 25 °C/min, respectively.

The DTG thermograms reveal two decomposition regimes in both samples for all the considered heating rates. The small peaks before 100 °C represent the evaporation of the adsorbed moisture in the samples, which can be dealt with by pretreatment before thermochemical or enzymatic conversion. The second major peak represents the α-cellulose in both samples. However, the α-cellulose derived from the date palm biomass decomposes at lower temperatures of 200–350 °C compared with the 280–370 °C of the commercial α-cellulose. Furthermore, for heating rates of up to 20 °C/min, the DTG thermograms of the commercial α-cellulose are slightly skewed to the right, indicating sensitivity to an increase in thermal energy. The difference between the decomposition temperatures of the commercial α-cellulose and that presently derived from date palm waste is attributable to their differing origins. The isolated cellulose and α-cellulose were further characterized by FTIR.

3.3. Fourier transform infrared (FTIR) spectroscopy

The FT-IR spectra of the celluloses isolated from the rachis, leaflet, and fiber of date palm waste in this study are shown in Figure 3(A) and (B). The purpose of the FTIR spectroscopy investigation was to determine the functional groups of the cellulose after removal of hemicellulose and lignin.

The vibrational band assignments are shown in Figure 3 (A). The FTIR spectroscopy results for the different date palm samples can be observed to be similar, indicating similar chemical compositions, as already suggested by the thermogravimetric analysis results. The broad absorption band observed between 3400 and 3500 cm^{-1} is attributable to the stretching vibration of the inter-hydrogen bonded OH group, while that around 2900 cm^{-1} is attributable to the CH groups of cellulose. Similar results were reported by Rosa et al. (2012) and Proniewicz et al. (2001) from their investigation of chlorine-free cellulose isolated from rice husk and whisker isolated from hydrothermally degraded cellulose, respectively. The strong peak around 1049 cm^{-1} is attributed to the stretching vibration of C–O–C in the pyranose skeletal ring, as also reported by Sun et al. (2004). Cellulose tends to be hydrophilic and thus strongly interacts with water on a molecular level. The peak absorption around 1645 cm^{-1} is thus assigned to OH bending in the water (Johar et al., 2012; Jonoobi et al., 2011). The bands around 1610 and 1344 cm^{-1} for the leaflet and fiber cellulose samples are assigned to CH_2 stretching of an aromatic ring and C–O stretching of an ether linkage, respectively. Viera et al. (2007) reported that the absence of the above bond vibrations in their characterization of methyl cellulose obtained from sugarcane bagasse cellulose was a confirmation of complete lignin removal. Their observation in the present study is thus attributed to the presence of residual lignin fractions in the leaflet and fiber cellulose samples. This small residual lignin fractions were also observed from the DTG thermograms (Figure 2 (A)) for the leaflet and fiber cellulose samples, although they were absent from the rachis cellulose sample. The absorption bands around 1735 cm^{-1} are assigned to C=O in either a ketone from the hemicellulose residue or due to partial acetylation of cellulose during the bleaching process, as has also been previously reported (Zuluaga et al., 2007; Sun et al., 2004).

Figure 3 (B) shows the FTIR spectra for the commercial α-cellulose and the present α-celluloses isolated from the different parts of date palm waste.

It can be seen from Figure 3 (B) that both the commercial and present α-celluloses have similar band absorptions at most wave lengths, indicating their possession of similar functional groups. However, there are also some noticeable differences; for example, the absence of C=O bond stretching around 1735 cm^{-1} in the commercial α-cellulose, as observed in the date palm α-celluloses, indicating the presence of residual hemicelluloses with C=O ketones absorbed around 1735 cm^{-1} (Sun et al., 2004). The latter observation is plausibly due to the acetylation process with 20% acetic acid during the present laboratory extraction of α-cellulose.

The leaflet and fiber cellulose samples were found to generally have relatively strong band absorptions, while the rachis α-cellulose had an absorption strength comparable to that of the commercial α-cellulose, hence their similar bond structures. A scanning electron microscope was used to conduct a deeper examination of the surface morphologies of the cellulose samples.

3.4. Scanning electron microscopy (SEM)

Scanning electron microscopy was used to detect the differences between the surface morphologies of the cellulose samples isolated from the rachis, leaflet, and fiber of date palm biomass in this study. Prior to the SEM analysis, the samples were coated with Au/C using a vacuum sputter coater to improve their conductivity and the quality of the obtained images. Figure 4 (X) and (Y) shows the SEM images of the celluloses isolated from the different parts of the date palm biomass.

The SEM micrographs in Figure. 4 (X); (a)–(c) reveal obvious differences between the morphologies of the celluloses isolated from the different parts of the date palm waste. The micrographs were obtained using a high magnification, and Figure. 4 (X); (a) and (c) show that the cellulose isolation produced skeletal rod-like macrofibril structures with an identifiable shape and comparable thickness and intra-fibrillar diameters. The well-defined cylindrical rod-like structures observed in the rachis and fiber celluloses can be described as highly porous with an appreciable diameter, thus capable of providing a large surface area for chemical and physical interactions and electronic conduction. However, the SEM micrographs of the leaflet cellulose (Figure 4 (X); (b)) reveals aggregated structures with no definite measurable length or diameter.

Figure 4 (Y) (a)–(d) show the SEM images of the α-celluloses isolated from the different parts of the date palm waste and the commercial α-cellulose, respectively.

It can be seen from Figure. 4 (Y); (a)–(c) that the α-celluloses derived from the rachis, leaflet, and fiber parts of the date palm biomass have non-uniform macrofibril shapes and distributions with intertwined morphologies. The same applies to the commercial α-celluloses. However, it was noted that the α-celluloses isolated from the date palm waste had some nodular agglomerates on their surfaces, not observed on the commercial sample. The nodular agglomerates were also observed in the SEM images obtained by Alawar et al. (2009), who characterized treated date palm fibers for use as composite reinforcement. However, no such nodular agglomerates were observed by Ovando-Medina et al. (2015), who synthesized an α-cellulose composite for use in removing reactive red dye from an aqueous solution. The SEM images reported by these previous researchers were like those of the commercial α-cellulose above, suggesting similar sources of the materials. The crystal structures of the present cellulose and α-cellulose samples were examined by XRD analysis.

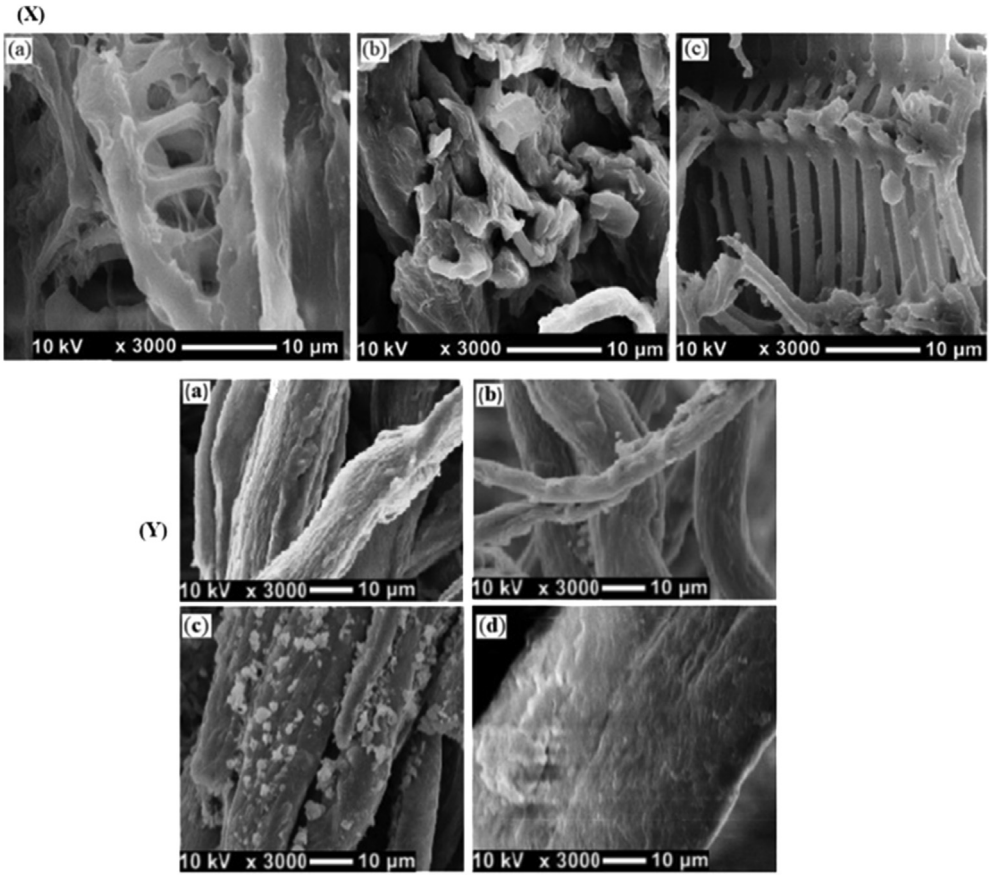

Figure 4. (X) and (Y) SEM images of the date palm celluloses and α-celluloses isolated from the (a) rachis, (b) leaflet, (c) fiber and (d) the commercial α-cellulose.

3.5. X-ray diffraction (XRD) analysis

Figure 5 (A) and (B) shows the XRD spectra of the celluloses isolated from the rachis, leaflet, and fiber of the date palm waste.

From Figure 5 (A), it can be observed that the major crystalline peak for each sample occurs around $2\theta = 22^{\circ}$, which represents the cellulose crystallographic plane (index = 200). Similar results were reported by Rosa et al. (2012) for chlorine-free cellulose extracted from rice and whisker. The crystallinity index (CI) was calculated for the different cellulose samples using the Segal formula in Eq. (1). The results are presented in Table 2 (see supplementary file; Table 2) Sheriff and Abdullah, 2013. The Segal formula is one of the most commonly used and easiest techniques for calculating the crystallinity index at the peak height of a crystalline material (Segal et al., 1959).

The investigated date palm parts had relatively high crystallinity indexes, with an average value of 52.27%. The present results are

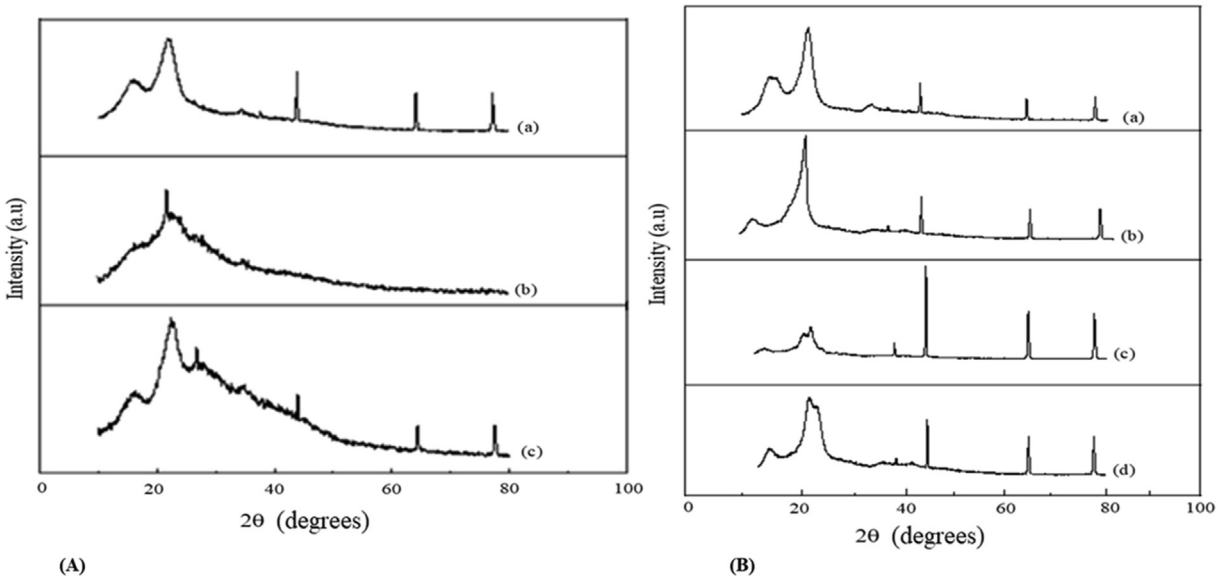

Figure 5. (A) and (B) cellulose XRD spectra of; (a) rachis, (b) leaflet, and (c) fiber, and α-cellulose of; (a) commercial and isolated (b) rachis, (c) leaflet, and (d) fiber.

comparable with those in the literature. For example, Abe and Yano (2009) reported crystallinity indexes of 68% and 71% for celluloses extracted from potato tuber and rice straw, respectively. Date palm waste can thus be used to replace some of the first-generation biomasses as raw materials to produce polymeric materials, composites, and other value-added products.

As shown in Figure 5(B), the extracted α-celluloses also have highly crystalline structures. All the α-celluloses obtained from the different date palm parts and the commercial α-cellulose have similar crystalline structures. The major crystalline and amorphous peaks occur around $2\theta = 22^{\circ}$ and between 2θ values of 15° and 18°, respectively. The calculated crystallinity indexes of the α-cellulose samples are presented in Table 3 (see supplementary file; Table 3). The improved crystallinities relative to those of the corresponding date palm biomass parts is an indication of the removal of hemicellulose and lignin. Hai et al. (2017) reported α-cellulose crystallinity indexes of soft wood and cotton within 50%–65 %. Park et al. (2014), who investigated the crystallinity variations of cotton linter caused by electron beam irradiation and acid treatment, reported α-cellulose crystallinity indexes within 98.1%–99.0 %.

It is noteworthy that both the cellulose and α-cellulose samples have additional crystal lattices at 42°, 65°, and 79°. These peaks have also been observed in the XRD results for bacterial cellulose/silver nanocomposites (Zhijiang et al., 2011). The resultant higher crystallinity increases the structural performance of the materials, enhancing their rigidity and stiffness. This improves the resistance of the materials to cracking, and hence their mechanical properties. The crystal lattice and high crystallinity of the isolated date palm celluloses and α-celluloses thus promise to enable the development of nanocomposites with improved mechanical properties. The particularly high crystallinity indexes of the date palm α-celluloses imply that they can compete with those extracted from other biomasses for utilization in biorefineries and other applications.

4. Statistical analysis

The Minitab software was used to conduct a statistical analysis of the results of this study using a general factorial regression design. Models for optimizing the cellulose and α-cellulose isolation processes based on certain identified factors were also developed (see supplementary statistical data and plots).

To analyze how the cellulose yield is determined, three factors, namely, the NaOH concentration, particle size, and part of date palm biomass, were varied as 0.1, 0.5, and 1 M; 180, 250, and 300 μm; and rachis (denoted by 1), leaflet (denoted by 2), and fiber (denoted by 3), respectively. An analysis of variance performed on the results obtained for various combinations of these factors revealed a 0.05% significance level, with a model F-value of 9.37 and p-value of 0.002. This implied a direct relationship between the cellulose yield and the considered factors. All the factors were also determined to be individually significant. However, the two-way and three-way interactions among the factors were not significant, as also attested to by the Pareto plots. It should be noted that a p value of <0.0500 indicates significant model terms. The model had $R^2 = 95.47\%$, which suggests that 95.47% of the yield can be explained by the three factors considered in the design, with the remaining 4.53% explained by other factors. The normality, constant variance, and independence residual plots revealed nothing unusual in the residuals. A regression equation for yield prediction was also obtained, as presented supplementary material on the statistical results. A process optimization was performed using a contour plot, surface plot, and optimization plot to ascertain the optimal operating conditions. The obtained optimization plots showed that achieving the highest possible cellulose yield of 74.7 % required the use of a low NaOH concentration of 0.1 M, a small particle size of 180 μm, and the rachis part of date palm biomass. These results formed the basis of the conditions used in this study, as discussed in the method section.

A two-factor statistical analysis considering the date palm biomass part and particle size, which were varied as mentioned above, was also conducted to examine the impact on the α-cellulose yield. The analysis of variance results for a 95% confidence interval (0.05% significance level), revealed a model F-value of 29.38 and p-value of 0.003. This implies that there is only a 0.3% chance that a model F-value this large could explain the relationship between the response and predictors considered in the design. All the factors were found to be significant. However, the two-way and three-way interactions were not significant, as also attested to by the Pareto plots. The model had $R^2 = 96.71\%$, which suggests that 96.71% of the yield could be explained by the two factors, and only 3.29% by other factors. The normality, constant variance, and independence residual plots revealed nothing unusual in the residuals. A regression equation for yield prediction as also derived, as presented in the supplementary material. A process optimization was conducted using a contour plot, surface plot, and optimization plot to determine the optimal operating conditions. The results showed that the achievement of the highest α-cellulose yield of 78.63% required the use of a small particle size of 180 μm and date palm rachis.

The results of the statistical analyses agree with those of the experiments, suggesting that cellulose isolation from date palm rachis afforded a higher yield compared with the use of other parts of the biomass, and that cellulose and α-cellulose could be isolated using a small particle size and low-concentration alkali treatment.

5. Conclusion

Low-concentration acid-alkali treatment and bleaching were successfully used to isolate cellulose and α-cellulose from different parts of lignocellulosic date palm waste, namely, rachis, leaflet, and fiber. The non-cellulosic fractions of the date palm biomass (hemicellulose and lignin) were removed in the process. The rachis part yielded the highest amounts of cellulose and α-cellulose, as attested to by both the experiments and statistical design. The characterization of the α-cellulose obtained from rachis revealed properties similar to those of commercial α-cellulose. The extracted cellulose and α-cellulose both exhibited relatively high crystallinity, demonstrating the potential of date palm waste for use as a biorefinery raw material. SEM analyses of the fiber cellulose revealed special surface morphologies comprising rod-like structures. Cellulose derived from date palm fiber thus has a potential utilization in the production of cellulose nanocrystals, which are an important component of reinforcement fillers used in polymer and other industries.

However, the crystallinity indexes of the α-celluloses obtained in this study may be considered as arbitrary values owing to a drawback of the employed Segal formula, which assumes that amorphous cellulose produces its main reflection at $2\theta = 18^{\circ}$, whereas it was observed at $2\theta = 16^{\circ}$ in the present study. There is thus the need for further investigation to determine the exact crystallinity indexes of the extracted α-celluloses. Nevertheless, the successful isolation and characterization of cellulose and α-cellulose from date palm waste in this study demonstrates the potential of the biomass to contribute to sustainable green growth, especially through its utilization as feedstock in biorefineries.

Declarations

Author contribution statement

Emmanuel Galiwango: Conceived and designed the experiments; Performed the experiments; Analyzed and interpreted the data; Contributed reagents, materials, analysis tools or data; Wrote the paper.

Nour S. Abdel Rahman: Performed the experiments.

Ali Al-Marzouqi: Conceived and designed the experiments; Analyzed and interpreted the data; Contributed reagents, materials, analysis tools or data.

Mahdi Abu-Omar: Contributed reagents, materials, analysis tools or data.

Abbas Khaleel: Analyzed and interpreted the data; Contributed reagents, materials, analysis tools or data.

Funding statement

This work was supported by the Emirates Center for Energy and Environment Research (grant numbers 31R107).

Competing interest statement

The authors declare no conflict of interest.

Additional information

Supplementary content related to this article has been published online at https://doi.org/10.1016/j.heliyon.2019.e02937.

Acknowledgements

The authors thank Mr. Bassam of the Department of Chemistry, United Arab Emirates University for granting access to the FTIR equipment used in this study.

References

Abe, K., Yano, H., 2009. Comparison of the characteristics of cellulose microfibril aggregates of wood, rice straw and potato tuber. Cellulose 16, 1017–1023.
Ahmed, I.A., Ahmed, A.W.K., Robinson, R.K., 1995. Chemical composition of date varieties as influenced by the stage of ripening. Food Chem. 54, 305–309.
Alawar, A., Hamed, A.M., Al-Kaabi, K., 2009. Characterization of treated date palm tree fiber as composite reinforcement. Composites Part B 40 (7), 601–606.
Aldrich, Sigma, 2019. α-Celluloses. www.sigmaaldrich.com. (Accessed 29 January 2019).
Alemdar, A., Sain, M., 2008. Isolation and characterization of nanofibers from agricultural residues – wheat straw and soy hulls. Bioresour. Technol. 99 (6), 1664–1671.
Brinchi, L., Cotana, F., Fortunati, E., Kenny, J.M., 2013. Production of nanocrystalline cellulose from lignocellulosic biomass: technology and applications. Carbohydr. Polym. 94 (1), 154–169.
Chen, Y.W., Lee, H.V., Abd Hamid, S.B., 2017. Facile production of nanostructured cellulose from elaeis guineensis empty fruit bunch via one pot oxidative-hydrolysis isolation approach. Carbohydr. Polym. 157, 1511–1524.
Ching, Y.C., Ng, T.S., 2014. Effect of preparation conditions on cellulose from oil palm empty fruit bunch fiber. Bioresources 9 (4), 6373–6385.
Das, K., Ray, D., Bandyopadhyay, N.R., Sengupta, S., 2010. Study of the properties of microcrystalline cellulose particles from different renewable resources by XRD, FTIR, nanoindentation, TGA and SEM. J. Polym. Environ. 18 (3), 355–363.
Emmanuel, G., Nour, S.A.R., Ali, H.A., Mahdi, M.A., Abbas, A.K., 2018. Klason method: an effective method for isolation of lignin fractions from date palm biomass waste. Chem. Process Eng. Res. 57, 46–58, 2225-0913.
Hai, L.V., Kim, H.C., Kafy, A., Zhai, L., Kim, J.W., Kim, J., 2017. Green all-cellulose nanocomposites made with cellulose nanofibers reinforced in dissolved cellulose matrix without heat treatment. Cellulose 24, 3301–3311.
Jiang, M., Zhao, M., Zhou, Z., Huang, T., Chen, X., Wang, Y., 2011. Isolation of cellulose with ionic liquid from steam exploded rice straw. Ind. Crops Prod. 33 (3), 734–738.
Johar, N., Ahmad, I., Dufresne, A., 2012. Extraction, preparation and characterization of cellulose fibers and nanocrystals from rice husk. Ind. Crops Prod. 37, 93–99.
John, O.B., Royal, H.R., 1931. The determination of the alpha-cellulose content and copper number of paper. Bur. Stand. J. Res. 6, 603–619.
Jonoobi, M., Khazaeian, A., Tahir, P.M., Azry, S.S., Oksman, K., 2011. Characteristics of cellulose nanofibers isolated from rubberwood a nd empty fruit bunches of oil palm chemo-mechanical process. Cellulose 18, 1085–1095.
Kumar, R., Sharma, R.K., Singh, A.P., 2017. Cellulose based grafted biosorbents - journey from lignocellulose biomass to toxic metal ions sorption applications - a review. J. Mol. Liq. 232, 62–93.
Loof, D., Hiller, M., Oschkinat, H., Koschek, K., 2016. Quantitative and qualitative analysis of surface modified cellulose utilizing TGA-MS. Materials 9 (6), 415.
Miranda, M.I.G., Bica, C.I.D., Nachtigall, S.M.B., Rehman, N., Rosa, S.M.L., 2013. Kinetical thermal degradation study of maize straw and soybean hull celluloses by simultaneous DSC–TGA and MDSC techniques. Thermochim. Acta 565, 65–71.
Nuruddin, M., Hosur, M., Uddin, M.J., Baah, D., Jeelani, S., 2016. A novel approach for extracting cellulose nanofibers from lignocellulosic biomass by ball milling combined with chemical treatment. J. Appl. Polym. Sci. 133 (9).
Ovando-Medina, V.M., Vizcaíno-Mercado, J., González-Ortega, O., Rodríguez de la Garza, J.A., Martínez-Gutiérrez, H., 2015. Synthesis of α-cellulose/polypyrrole composite for the removal of reactive red dye from aqueous solution: kinetics and equilibrium modeling. Polym. Compos. 36 (2), 312–321.
O'Sullivan, A.C., 1996. Cellulose: the structure slowly unravels. Blackie Acad Prof 4, 173–207.
Park, H.J., Sohn, H.N., Seo, Y.B., 2014. Cotton linter crystallinity variations caused by electron beam irradiation and acid treatment. J. Korea Tech. Assoc. Pulp Pap. Ind. 46 (4), 37–43.
Prakash, O., Naik, S., Naik, M., Katiyar, R., Kumar, D., Maji, D., et al., 2018. Novel process for isolation of major bio-polymers from mentha arvensis distilled biomass and saccharification of the isolated cellulose to glucose. Ind. Crops Prod. 119, 1–8.
Proniewicz, L.M., Paluszkiewicz, C., Wesełucha-Birczyńska, A., Majcherczyk, H., Barański, A., Konieczna, A., 2001. FT-IR and FT-Raman study of hydrothermally degradated cellulose. J. Mol. Struct. 596 (1–3), 163–169.
Reyes-Luyanda, D., Flores-Cruz, J., Morales-Pérez, P.J., Encarnación-Gómez, L.G., Shi, F., Voyles, P.M., Cardona-Martínez, N., 2012. Bifunctional materials for the catalytic conversion of cellulose into soluble renewable biorefinery feedstocks. Top. Catal. 55 (3), 148–161.
2011 Rosa, S.M.L., Rehman, N., de Miranda, M.I.G., Nachtigall, S.M.B., Bica, C.I.D., 2012. Chlorine-free extraction of cellulose from rice husk and whisker isolation. Carbohydr. Polym. 87 (2), 113–1138.
Segal, L., Creely, J.J., Marin, A.E., Conrad, C.M., 1959. An empirical method for estimating the degree of crystallinity of native cellulose using the x-ray diffractometer. Text. Res. J. 29, 786–794.
Sheltami, R.M., Abdullah, I., Ahmad, I., Dufresne, A., Kargarzadeh, H., 2012. Extraction of cellulose nanocrystals from mengkuang leaves (pandanus tectorius). Carbohydr. Polym. 88 (2), 772–779.
Sheriff, M.A.S.K., Abdullah, G.A., 2013. New composite based on starch and mercerizing cellulose. Am. J. Polym. Sci. 3 (3), 46–51.
Sun, X., Sun, R., Su, Y., Sun, J., 2004. Comparative study of crude and purified cellulose from wheat straw. J. Agric. Food Chem. 52 (4), 839–847.
Szymańska-Chargot, M., Chylińska, M., Gdula, K., Kozioł, A., Zdunek, A., 2017. Isolation and characterization of cellulose from different fruit and vegetable pomaces. Polymers 9 (10), 495.
Viera, R.G.P., Filho, G.R., de Assunção, R.M.N., Meireles, C.S., Vieira, J.G., de Oliveira, G.S., 2007. Synthesis and characterization of methylcellulose from sugar cane bagasse cellulose. Carbohydr. Polym. 67 (2), 182–189.
Wu, S., Shen, D., Hu, J., Zhang, H., Xiao, R., 2016. Cellulose-lignin interactions during fast pyrolysis with different temperatures and mixing methods. Biomass Bioenergy 90, 209–217.
Yang, S., Zhang, Y., Yue, W., Wang, W., Wang, Y., Yuan, T., Sun, R., 2016. Valorization of lignin and cellulose in acid-steam-exploded corn stover by a moderate alkaline ethanol post-treatment based on an integrated biorefinery concept. Biotechnol. Biofuels 9 (1), 9–238.
Zaid, I., Helal, H.A., 2000. Date palm Research and Development Program. United Nations Office for Project Services, 002.
Zhang, Y.-H.P., Lynd, L.R., 2006. A functionally based model for hydrolysis of cellulose by fungal cellulase. Biotechnol. Bioeng. 94, 888–898.
Zhijiang, C., Chengwei, H., Guang, Y., Jaehwan, K., 2011. Bacterial cellulose as a template for the formation of polymer/nanoparticle nanocomposite. J. Nanotechnol. Eng. Med. 2 (3), 31006.
Zuluaga, R., Putaux, J.L., Restrepo, A., Mondragon, I., Ganan, P., 2007. Cellulose microfibrils from banana farming residues: isolation and characterization. Cellulose 14, 585–592.